# High-resolution three-dimensional imaging of islet-infiltrate interactions based on optical projection tomography assessments of the intact adult mouse pancreas

**Tomas Alanentalo**
**Christina E. Lorén**
Umeå University
Umeå Centre for Molecular Medicine
S-901 87, Umeå, Sweden

**Åsa Larefalk**
Umeå University
Dept. of Medical and Clinical Genetics
S-901 85, Umeå, Sweden

**James Sharpe**
ICREA and EMBL-CRG Systems Biology Program
Centre for Genomic Regulation
Dr. Aiguader 88, 08003, Barcelona, Spain

**Dan Holmberg**
Umeå University
Dept. of Medical and Clinical Genetics
S-901 85, Umeå, Sweden

**Ulf Ahlgren**
Umeå University
Umeå Centre for Molecular Medicine
S-901 87, Umeå, Sweden

**Abstract.** A predicament when assessing the mechanisms underlying the pathogenesis of type-1 diabetes (T1D) has been to maintain simultaneous global and regional information on the loss of insulin-cell mass and the progression of insulitis. We present a procedure for high-resolution 3-D analyses of regions of interest (ROIs), defined on the basis of global assessments of the 3-D distribution, size, and shape of molecularly labeled structures within the full volume of the intact mouse pancreas. We apply a refined protocol for optical projection tomography (OPT)-aided whole pancreas imaging in combination with confocal laser scanning microscopy of site-directed pancreatic microbiopsies. As such, the methodology provides a useful tool for detailed cellular and molecular assessments of the autoimmune insulitis in T1D. It is anticipated that the same approach could be applied to other areas of research where 3-D molecular distributions of both global and regional character is required.  [DOI: 10.1117/1.3000430]

Keywords: optical projection tomography; confocal microscopy; pancreas; microbiopsy; insulitis; diabetes.

Paper 08180LR received Jun. 12, 2008; revised manuscript received Aug. 10, 2008; accepted for publication Sep. 8, 2008; published online Oct. 29, 2008.

## 1 Introduction

Many areas of biomedical research have been held back by limited possibilities to extract simultaneous global and regional information of a studied biological process or event. Commonly, high-resolution studies of specific cell niches or regions of interest (ROIs) within a greater body of tissue does not allow for the resultant data to be put into a larger context. Due to technical limitations, information on spatial origin of the studied region, neighboring cell types, and the global state of the organ studied is often lost. Conversely, technologies allowing whole organ imaging do not generally provide the resolution required for detailed cell-level analyses. A protocol allowing for high-resolution analysis to be directed by a prior global assessment of the disease state of an entire organ would thus constitute a significant asset for many areas of research. A good example comes from different murine models for development of type-1 diabetes (T1D). Our present understanding of the natural history of this disease[1] rests to a large extent on analysis of rodent models, in particular the nonobese diabetic (NOD) mouse.[2,3] This model is characterized by the autoreactive T-cell mediated destruction of pancreatic $\beta$-cells, leading to diabetes.[4–6] While it is well established that insulitis progresses over an extended time period, detailed understanding of its kinetics, as well as the cellular and molecular mechanisms underlying observed regional variations, is largely lacking due to limitations in existing technology. In particular, high-magnification imaging alone [e.g., confocal laser scanning microscopy (CLSM) on isolated islets of Langerhans[7]], while providing excellent details about individual islets, does not provide an overview of disease progression at the level of the whole pancreas. Further, it does not generate information regarding the spatial origin of the analyzed islet, and importantly, does not permit studies of neighboring/interacting cell types and molecules.

We have previously adapted the concept of optical projection tomography (OPT)[8,9] to allow for imaging of specifically labeled structures within intact mouse organs, including the pancreas.[10] To develop a means by which both the details of the autoimmune attack at the islet level, and also information of the global state of the pancreatic gland, could be studied in

Address all correspondence to Dan Holmberg, Tel: 46-90-785-4407, E-mail: Dan.Holmberg@medbio.umu.se; or Ulf Ahlgren, Tel: 46-90-785-4434, Fax: 46-90-785-4400, E-mail: Ulf.Ahlgren@ucmm.umu.se.

1083-3668/2008/13(5)/054070/4/$25.00 © 2008 SPIE

the same specimen, we postulated that four criteria would have to be met. The methodology should allow for; 1. global (whole organ) assessments of molecularly labeled pancreatic constituents (e.g., insulin producing islets); 2. selection of ROIs based on the expression of specific markers and the spatial position, shape, and size of individual objects; 3. high resolution analyses of user-defined ROIs identified based on the global assessment; and 4. high resolution 2-D and 3-D analyses of two or more molecular markers within the ROI. To develop a protocol that would meet these criteria, we turned to the NOD mouse model for T1D.

## 2 Experimental Methods

### 2.1 *Animals and Organ Preparation*

Intact female NOD pancreata from our local breeding colony (NOD/Bom) were isolated at week 16 and stained for insulin as described.[10] All animals used in this study were used with approval of the Ethical Committee on Animal Experiments for Northern Sweden.

### 2.2 *Optical Projection Tomography*

OPT scanning was performed using the Bioptonics 3001 OPT scanner (Bioptonics, Edinburgh, United Kingdom) modified with an exciter D560/40× and emitter E610lpv2 filter (Chroma, Rockingham, Vermont), which significantly improved the signal-to-noise ratio and obviated the use of the background subtraction protocol previously applied for assessing $\beta$-cell mass.[10] Scans were performed with an in-house modified mount that could better bear the weight of the adult pancreatic specimen. Tomographic reconstructions were generated using the NRecon V1.5.0 (SkyScan, Kontich, Belgium) software, orthogonal planes were assessed using DataViewer V1.3.2 (SkyScan), and volume renderings were created using Bioptonics Viewer V1.61 (Bioptonics). Islet $\beta$-cell volumes were quantified using a measurement protocol created in the quantification software module for Volocity v4.3.2 (Improvision, Coventry, United Kingdom). Image stacks of tomographic sections were manually edited to remove any reconstruction artifacts (e.g., the occasional apparent merging of large islets located very close to each other). Thereafter, a "find objects by intensity" task was applied to the measurement protocol. This protocol selects voxels according to specified intensity threshold values. This value was manually edited to exclude pixels with intensity values lower than those normally contributing the labeled objects (islets). Next, a fine filter (3 $\times$3 kernel) was applied to avoid selection of voxels not contributing to individual islets. Potential artifacts such as dust particles were identified in interactive 3-D models and deselected from the measurements window. Measured objects were finally exported to the Excel 2007 (Microsoft Corporation, Redmond, Washington) software for statistical analysis.

### 2.3 *Isolation of Biopsies*

Scanned pancreatic specimens were immersed in Murrays clear benzyl alcohol (AL0161, Scharlau, Barcelona, Spain): [Benzyl benzoate (154839, MP Biomedicals, Illkirch, France) in a 1:2 ratio] in a glass petri dish and labeled objects (islets) were visualized in a Nikon SMZ800 stereo microscope equipped for fluorescence using an EX 560/40, DM 595/ EM 630/60 filter set. Guided by interactive volume reconstructions, ROIs selected on islet morphology, size, 3-D distribution, or all parameters combined, could be easily located. ROIs were carefully isolated as biopsies from the agarose embedded specimen using glass capillaries (1-mm inner diameter) whose ends had been ground sharp using an Arkansas stone. The isolated biopsies were washed in methanol, rehydrated into Tris buffered Triton x-100 supplemented saline, and immunostained with a marker for infiltrating T lymphocytes (CD3). Antibodies used were rabbit anti-CD3 (C7930, 1:200, Sigma, St. Louis, Missouri) and Alexa 488 goat anti-rabbit (1:500, Invitrogen, Carlsbad, California). Thereafter, the biopsies were dehydrated in methanol, cleared in Murray's clear, and transferred to 1-mm-deep microwells for confocal scanning. ROI biopsies were analyzed on a Nikon C1 confocal microscope fitted with argon (488 nm) and a helium/neon (594 nm) laser. Samples were scanned through a Nikon Plan Fluor 20$\times$0.75 Mlmm objective. Companion images were scanned at 512$\times$512 pixels and 0.65-$\mu$m step size. Volume, isosurface, and wire-frame renderings were generated using the Imaris v3.3.2 software (Bitplane, Zurich, Switzerland).

## 3 Results

*Obtaining parameters for region-of-interest selection.* The OPT scan data [Fig. 1(a)] were reconstructed providing tomographic sections throughout the volume of each pancreas [Figs. 1(a) through 1(g), 1(i), and 1(j) and other data not shown]. 3-D volume reconstructions were subsequently generated based on the signal from the insulin-specific antibodies and from tissue autofluorescence [Fig. 1(b)]. These are fully interactive and allow for free tilting, zoom, and virtual clipping of the specimen (Video 1). Based on the tomographic data, specific islet $\beta$-volumes were quantified. This generated a full histogram of islet $\beta$-cell volumes and information of corresponding centroid coordinates [Fig. 1(h) and other data not shown]. In the example depicted in Fig. 1(b), the pancreas (16 week duodenal-NOD) contained 93 insulin labeled islets having islet $\beta$-cell volumes ranging from $2.9\times10^3$ $\mu$m$^3$ (which equals the maximum spatial resolution for the current sample at utilized zoom factor) to $2.56\times10^7$ $\mu$m$^3$ [Fig. 1(h)]. The total islet $\beta$-cell volume for the current specimen was $3.46\times10^8$ $\mu$m$^3$. As compared to stage matched NOD H2b congenic pancreata, this volume corresponds to approximately a 50% reduction in insulin cell mass. The control specimen depicted in Figs. 1(i) and 1(j) contained 1063 islets with a total $\beta$-cell volume of $6.73\times10^8$ $\mu$m$^3$.

*Isolation of regions of interest.* To address the spatial character of infiltrating cell types, individual islets were selected based on their position within the whole pancreas (e.g., peripheral location or near the main duct), their shape (e.g., spherical or elongated), or their size. In the current example, two neighboring islets with different shapes and volumes were selected [smaller elongated (assigned yellow pseudocolor in Fig. 1(b)) and dumbbell-shaped larger (assigned red pseudocolor in Fig. 1(b))]. 3-D quantification of the two islets provided information of their individual $\beta$-cell volume. In the current example, the "red" islet $\beta$-cell volume was $2.56\times10^7$ $\mu$m$^3$ and the spherical "yellow" islet $1.04\times10^7$ $\mu$m$^3$.

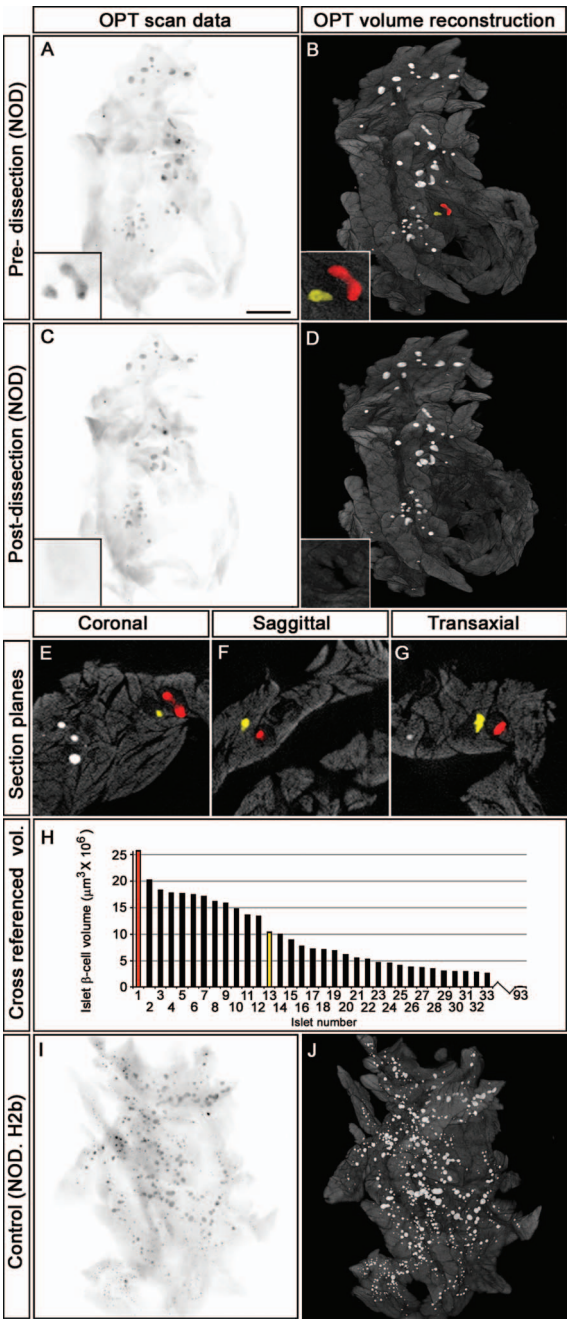


**Fig. 1** ROIs can be selected at will within the entire volume of the intact pancreas based on the spatial position, shape, and volume of specifically labeled objects. (a) and (c) show single images from the OPT scan datasets before (a) and after (c) microdissection of the selected ROI (insets). (b) and (d) show volume reconstructions of the pancreas based on the background autofluorescence (dark gray) and the signal from insulin-specific antibodies (white-islets) before (b) and after (d) isolation of the ROI (insets). The selected islets have been assigned red and yellow pseudocolors. (e), (f), and (g) show orthogonal section planes depicting the selected islets (red and yellow) from (e) coronal, (f) saggittal, and (g) transaxial views. (h) Histogram of individual islet $\beta$-cell volumes. Volume data for the "red" and "yellow" islets depicted in, (b), (e), (f), and (g) have been assigned corresponding color codes. (i) and (j) show single images from (i) the OPT scan dataset and (j) corresponding volume reconstruction of a control NOD H2b pancreata. Scale bar in (a) is 2000 $\mu$m in (a) through (d), (i), and (j), inset 800 $\mu$m and 970 $\mu$m in (e), (f), and (g).

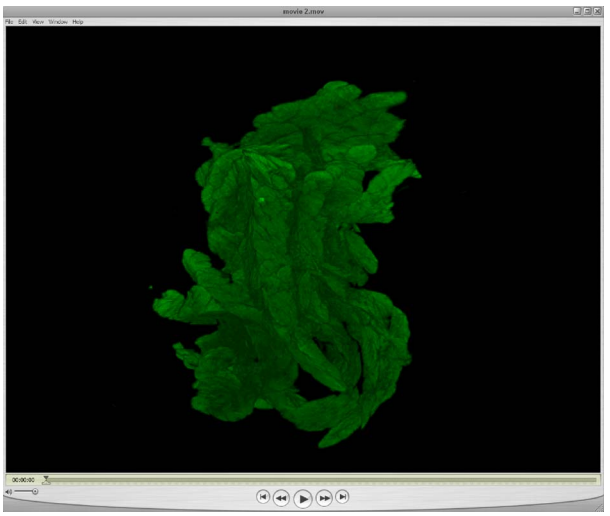

**Video 1** Interactive OPT-generated 3-D renderings facilitate identification and isolation of individual islets within the full volume of the pancreas. The movie shows a screen recording of the specimen seen in Fig. 1(a) and illustrates how volume renderings of pancreas specimen can be interactively manipulated to facilitate identification and isolation of specific ROIs. Here, the specimen is first rotated (aligned with the field of view in the stereomicroscope) and thereafter the background fluorescence channel (green) is made semitransparent to lay bare the insulin labeled islets (red). Finally, the magnification is increased (QuickTime, 4.8 MB).
[URL: http://dx.doi.org/10.1117/1.3000430.1]

Volumetric data could be cross-referenced back to the 3-D model and served as a converse selection criterion [red and yellow in Figs. 1(b) and 1(e) through 1(h)]. Although these data provide both global and regional information, the current resolution of the OPT technology does not permit cell-resolution analyses of individual islets when addressing specimens on a current scale. Selected islets were therefore isolated as microbiopsies, in the current example containing both the "red" and "yellow" islets. This was made possible by using the interactive volume reconstructions as reference guides to accurately guide the biopsy capillary into the fixed pancreas specimen [Video 1 and Fig. 2(a)]. After the biopsy was removed, the pancreas was subjected to another round of OPT scanning to confirm that the selected ROI had been properly isolated [Figs. 1(c) and 1(d)].

*Confocal analyses of regions of interest.* To address the amount and spatial distribution of infiltrating cell types in relationship to the selected islets, the biopsies were stained with antibodies against a marker for infiltrating T-lymphocytes (CD3), and CLSM scanned. This allowed for the generation of high-resolution orthogonal sections planes (data not shown) throughout the ROI (down to ~0.5-mm $z$ depth when using the 20× objective), as well as for the generation of volume-, isosurface-, and wire-frame renderings of the selected islet $\beta$-cell volumes and surrounding infiltrate [Figs. 2(b) through 2(k)], altogether facilitating a detailed 3-D assessment of the infiltration process (islets depicted correspond to the "red" and "yellow" islets in Fig. 1). In the current example, the two islets displayed insulitis varying from partly [Figs. 2(b) through 2(f)] to fully T-cell enclosed islets [Figs. 2(g) through 2(k)]. Comparing OPT with CLSM data of 24

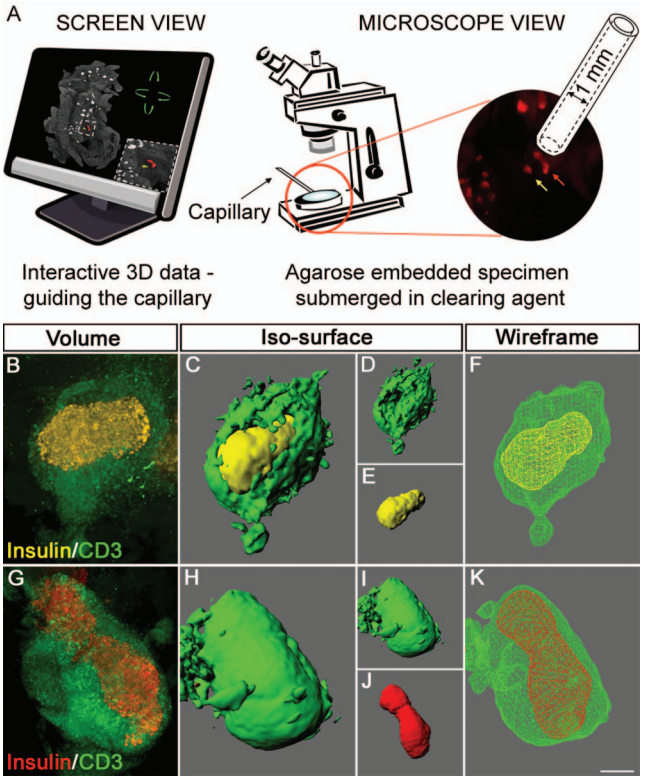


**Fig. 2** High-resolution 3-D assessment of two individual islets and interacting infiltrate. (a) Schematic illustrating the use of interactive OPT datasets for isolation of individual islets within the full volume of the pancreas. The interactive datasets allow for free rotation, zoom, and virtual clipping of the pancreas outline and the labeled islets. This facilitates the identification and isolation of individual islets in a view matching the field of view of the agarose-embedded specimen in the stereo microscope. (b) through (k) show CLSM data of the highlighted islets in Fig. 1. For each islet, (b) and (g) volumetric and (c) through (k) 3-D isosurface data are shown. In all cases, *green* represents the infiltrate (CD3), and the islet $\beta$-cell volumes (insulin) are shown as *yellow* or *red* to correspond with Fig. 1. In (f) and (k), the isosurfaces have been rendered as wire frames to facilitate a complete interpretation of the data. (For clarity, the wire frame renderings have been based on a larger voxel size to reduce the number of triangles). Note that a fiber in Fig. 1(g) has been digitally removed. Scale bar in (k) is 150 $\mu$m in (b), (c), and (f), 75 $\mu$m in (d) and (e), 100 $\mu$m in (g), (h), and (k), and 50 $\mu$m in (i) and (j).

islets indicated a 1-D variation of $\pm$3-5%, which translates into a volumetric variation of $\pm$10-15% per islet between the two techniques.

## 4 Discussion

In this study we provide a protocol that allows for site-directed analysis based on a global overview of the composition of the pancreas (i.e., volume and spatial distribution of molecularly labeled objects within the full volume of the gland). By applying this approach to the NOD model of type-1 diabetes, we demonstrate that all required criteria for such analyses have been fulfilled, and we provide detailed 3-D images of the autoimmune attack on individual islets of Langerhans. Although not falling within the scope of this brief work, it should be possible to expand these analyses to cover the infiltration dynamics of other subpopulations of the autoimmune attack during this process. Further, we anticipate that the developed methodology could easily be adapted to studies of combined global and region-specific character also in other organ systems, e.g., when high-resolution analyses of rare cell niches or events in a larger body of tissue are required.

### *Acknowledgments*

This work was supported by grants from the Swedish Research Council (Holmberg and Ahlgren), the Juvenile Diabetes Foundation (Sharpe, Holmberg, and Ahlgren), The Kempe Foundation, (Ahlgren), and Biotech Grants from the Umeå University Medical Faculty (Holmberg and Ahlgren).

### *References*

1. R. Gianani and, G. S. Eisenbarth, "The stages of type 1A diabetes," *Immunol. Rev.* **204**, 232–249 (2005).
2. M. S. Anderson and, J. A. Bluestone, "The NOD Mouse: a model of immune dysregulation," *Annu. Rev. Immunol.* **23**, 447–485 (2005).
3. S. Makino, K. Kunimoto, Y. Muraoka, Y. Mizushima, K. Katagiri, and Y. Tochino, "Breeding of a non-obese, diabetic strain of mice" *Jikken Dobutsu* **29**(1), 1–13 (1980).
4. H. S. Jun, C. S. Yoon, L. Zbytnuik, N. van Rooijen, and J. W. Yoon, "The role of macrophages in T cell-mediated autoimmune diabetes in nonobese diabetic mice," *J. Exp. Med.* **189**, 347–358 (1999).
5. P. Hoglund, J. Mintern, C. Waltzinger, W. Heath, C. Benoist, and D. Mathis, "Initiation of autoimmune diabetes by developmentally regulated presentation of islet cell antigens in the pancreatic lymph nodes," *J. Exp. Med.* **189**(2), 331–339 (1999).
6. K. U. Lee, K. Amano, and J. W. Yoon, "Evidence for initial involvement of macrophage in development of insulitis in, NOD. mice," *Diabetes* **37**(7), 989–991 (1988).
7. T. C. Brelje, D. W. Scharp, and R. L. Sorenson, "Three-dimensional imaging of intact isolated islets of Langerhans with confocal microscopy," *Diabetes* **38**(6), 808–814 (1989).
8. J. Sharpe, U. Ahlgren, P. Perry, B. Hill, A. Ross, J. Hecksher-Sorensen, R. Baldock, and D. Davidson, "Optical projection tomography as a tool for 3D microscopy and gene expression studies," *Science* **19**, 296(5567): 541–545 (2002).
9. J. Sharpe, "Optical projection tomography," *Annu. Rev. Biomed. Eng.* **6**, 209–228 (2004).
10. T. Alanentalo, A. Asayesh, H. Morrison, C. E. Loren, D. Holmberg, J. Sharpe and, U. Ahlgren, "Tomographic molecular imaging and 3D quantification within adult mouse organs," *Nat. Methods* **4**(1), 31–33 (2007).